sure 1.3 billion atoms of ^{231}Pa (500 fg, the amount in 0.5 g of coral in secular equilibrium) to ±0.5% (2σ). As a test of the accuracy of the tracer calibrations and the mass spectrometric measurements, each laboratory's tracer was used to calibrate a ^{231}Pa standard solution. The calibrations agreed.
14. R. L. Edwards, F. W. Taylor, G. J. Wasserburg, *Earth Planet. Sci. Lett.* **90**, 371 (1988).
15. J. L. Banner, G. J. Wasserburg, J. H. Chen, J. D. Humphrey, *ibid.* **107**, 129 (1991).
16. J. M. A. Chappell and H. A. Polach, *Quat. Res.* **2**, 244 (1972).
17. S. A. Wainwright, *Q. J. Micr. Sci.* **104**, 169 (1963); A. J. Ameil, D. S. Miller, G. M. Friedman, *Sedimentology* **20**, 523 (1973).
18. Each quoted age is the average of all ^{230}Th and ^{231}Pa ages for each sample with concordant ages. Each error is the error in ^{231}Pa age, which is, for each sample, larger than the error in ^{230}Th age. For samples with more than one ^{231}Pa age determination, the error was calculated by combining the errors quadratically and dividing by the number of ^{231}Pa age determinations. It is possible to have a concordant age even if the sample has behaved as an open system, if open-system behavior caused the isotopic composition to shift along concordia. An example of this type of behavior would be U loss for a material younger than 10,000 years. In this case, as the U is lost, the isotopic composition of the material will shift along a line with a slope very close that of concordia. In the case of the Barbados corals, all of the materials are significantly older than 10,000 years and would not be affected by this sort of artifact.
19. J. Imbrie *et al.*, in *Milankovitch and Climate*, A. Berger, J. Imbrie, G. Kukla, B. Saltzman, Eds. (Reidel, New York, 1984), part 1, pp. 269–306.
20. A. L. Berger, *Quat. Res.* **9**, 139 (1978); and tabulated values supplied by A. L. Berger.
21. J. Imbrie, A. C. Mix, D. Martinson, *Nature* **363**, 531 (1993).
22. Other questions regarding the accuracy of the Devils Hole chronology include the possibility that there was some initial ^{230}Th in the calcite resulting in artificially high ages [N. J. Shackleton, *Nature* **362**, 596 (1993); R. L. Edwards and C. D. Gallup, *Science* **259**, 1626 (1993)]. Recent data argue against this possibility [K. R. Ludwig, K. R. Simmons, I. J. Winograd, B. J. Szabo, A. C. Riggs, *Science* **259**, 1626 (1993)]. Another concern (*6*) was that if the growth rate of Devils Hole calcite varied, linear interpolation of ages between dated subsamples would lead to inaccuracy. Recent data again argue against this artifact (K. R. Ludwig, personal communication).
23. T. J. Crowley and K.-Y. Kim, *Science* **265**, 1566 (1994).
24. See, for example, W. R. Peltier and W. T. Hyde, *J. Atmos. Sci.* **44**, 1351 (1986).
25. We thank D. A. Pickett, who helped initiate this project; J. A. Hoff, for discussions and technical help; C. D. Gallup and R. G. Johnson, who helped with the Barbados field program; A. L. Bloom and J. M. A. Chappell, who led the 1988 field expedition to Papua New Guinea; C. Allegre, who brought the early Pa-Th concordia work to our attention; and K. R. Ludwig, I. J. Winograd, F. W. Taylor, Y. Asmerom, and R. K. Mathews, who contributed samples. This work was supported by the Donors of The Petroleum Research Fund, administered by the American Chemical Society; NSF grants OCE-9402693, OCE-9500647, EAR-9512334, and EAR-9406183 to R.L.E.; and a U.S. Department of Energy, Office of Basic Energy Sciences, Geosciences Research Program grant to M.T.M. and S.J.G.

30 December 1996; accepted 25 March 1997

Effect of Low Glacial Atmospheric CO_2 on Tropical African Montane Vegetation

Dominique Jolly* and Alex Haxeltine

Estimates of glacial-interglacial climate change in tropical Africa have varied widely. Results from a process-based vegetation model show how montane vegetation in East Africa shifts with changes in both carbon dioxide concentration and climate. For the last glacial maximum, the change in atmospheric carbon dioxide concentration alone could explain the observed replacement of tropical montane forest by a scrub biome. This result implies that estimates of the last glacial maximum tropical cooling based on tree-line shifts must be revised.

Atmospheric general circulation model simulations for the last glacial maximum (LGM; 18,000 ^{14}C years before the present) have been used to study the effects of low greenhouse gas concentration, extended ice-sheet distribution, and lowered sea-surface temperatures on climate and vegetation (*1*, *2*). Knowledge of tropical paleoclimates is crucial for evaluating the reliability of LGM climate model simulations, and such evaluations can check the models' ability to simulate future climates (*3*, *4*). Pollen data from East Africa have been used to estimate the climate of the tropics at the LGM (*5*–*7*). For the LGM, East African pollen records show that cool grassland and xerophytic scrub increased at the expense of tropical montane forests (*2*). However, the occurrence of trees such as *Podocarpus* and *Olea* in low abundances suggests that forest refuges persisted near some sites (*5*, *8*). Tree lines also dropped in elevation by about 1000 m. On the basis of analogs with modern pollen assemblages, these changes have been attributed to a combination of cooler (4°C lower) and drier (30% less precipitation) conditions at the LGM than at present (*9*, *10*). This magnitude of cooling was in better agreement with climate model simulations (*11*) than with empirical estimates derived from continental-scale paleoenvironmental data (*12*). Recent $\delta^{13}C$ measurements on glacial-age sediments from high-elevation sites indicate that C_4 plants were more abundant at the LGM than they are today. These data raise the possibility that the lowered atmospheric CO_2 concentration (*13*) may have influenced the vegetation through physiological effects (*14*). We used the vegetation model BIOME3 (*15*) to examine what changes in CO_2, temperature, and precipitation might account for the observed characteristics of East African montane vegetation at the LGM.

BIOME3 (*15*, *16*) is a process-based terrestrial biosphere model that simulates the interacting effects of climate and atmospheric CO_2 levels on vegetation distribution and biogeochemistry (*15*, *17*). The model includes a photosynthesis scheme that simulates acclimation of plants to changed atmospheric CO_2 levels by optimization of nitrogen allocation to foliage and by accounting for the effects of CO_2 on net assimilation, stomatal conductance, leaf area index, and ecosystem water balance (*18*).

The Kashiru site (in Burundi) provides a well-dated, high-resolution LGM pollen record (*8*). Today, the Kashiru peat bog is located in the potential afromontane forest zone and contains *Macaranga*, *Podocarpus*, *Olea*, *Syzygium*, Araliaceae, and *Entandrophragma* (*19*). During the LGM, the site was occupied by a xerophytic association (the ericaceous belt) dominated by Gramineae, Ericaceae, *Artemisia*, and temperate families such as Caryophyllaceae, Dipsacaceae, Cruciferae, and Ranunculaceae (*8*).

We obtained current climate data for the 0.5° grid cell containing Kashiru (13°28′S, 29°34′E, 2240-m elevation) from an updated version of a global climate database (*20*). The monthly mean climate values were adjusted to be consistent with available data (*9*) on annual mean temperature and precipitation at Kashiru (15.8°C and 1460 mm/year). We assumed that the soils have a medium texture. Atmospheric pressure was estimated as 7.7×10^4 Pa (*21*) and was used to calculate the partial pressures of O_2 and CO_2. Absolute minimum temperature was estimated from a global regression of absolute minimum temperature on mean temperature of the coldest month (*22*).

A simulation with the preindustrial atmospheric CO_2 level (*23*) and present climate (Fig. 1A) resulted in tropical montane forest (dominated by broad-leaved evergreen trees) at the Kashiru site, consistent with the present natural vegetation. A transition to evergreen microphyllous (ericaceous) scrub, similar to the LGM vegetation, was predicted when annual temperature was reduced by a minimum of 6.5°C. A

Global Systems Group, Department of Ecology, Lund University, Ecology Building, S-223 62 Lund, Sweden.

*To whom correspondence should be addressed. E-mail: djolly@planteco.lu.se

decrease in precipitation of up to 50% (730 mm/year) caused no change in biome, indicating that the current moisture supply is not limiting to vegetation. As the atmospheric CO_2 level was reduced, the minimum temperature reduction (from present) required for a transition from forest to scrub biomes decreased in magnitude (Fig. 2).

When the atmospheric CO_2 concentration in the model was lowered to the LGM value of 190 ppmv (*13*), a scrub biome replaced the montane forest, even with the present temperature and precipitation values (Fig. 1B). A combination of LGM CO_2 concentration, lowered precipitation, and present-day temperatures resulted in the prediction of a savanna (with co-dominant C_4 grasses), instead of forest or scrub. Thus, we infer that a large (>25%) reduction in precipitation must have been accompanied by a cooling of at least 1.5°C in order for woody plants to be dominant. With the preindustrial atmospheric CO_2 level, BIOME3 simulated a tree line occurring at an annual temperature 6.5°C less than the current annual temperature at Kashiru; starting with the elevation of the Kashiru site (2240 m) and a lapse rate of 0.54°C per 100 m (*24*), our simulation gave a predicted tree line at 3440 m. This is in agreement with the observed modern forest limit, which occurs between 2900 and 3400 m in this region (*25*).

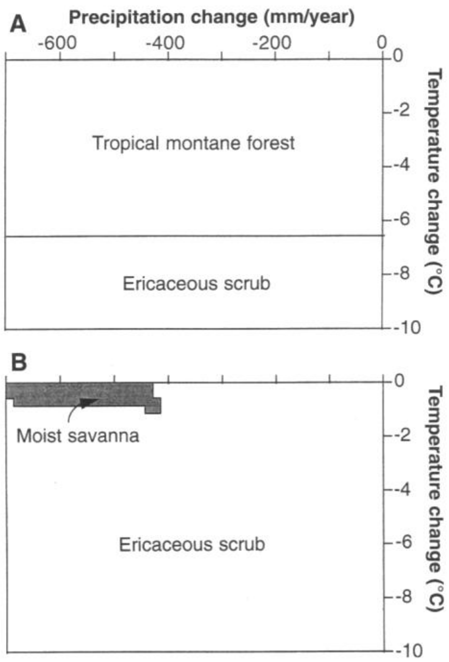

Fig. 1. Biomes simulated by BIOME3 (*15*) at Kashiru (13°28′S, 29°34′E, 2240 m elevation) for the present climate (with mean annual temperature of 15.8°C and mean annual precipitation of 1460 mm/year) and with a lowered temperature and precipitation. Results are shown for (**A**) the preindustrial (280 ppmv) (*23*) and (**B**) LGM (190 ppmv) (*13*) CO_2 concentrations. The seasonality of temperature and precipitation was held constant for the sensitivity analysis.

Initial estimates of the LGM climate in East Africa interpreted the tree-line depression as solely due to lowered temperature. The cooling was estimated to be 6°C (*26*). This is consistent with our findings (6.5°C) if the change in vegetation is attributed to temperature alone. However, the existence of a CO_2 effect implies that the cooling may have been less. More recent reconstructions of LGM climate from pollen data allow for the combined effects of low temperatures and low precipitation (*9*, *10*), but these, too, neglect CO_2 effects.

The strong effect of CO_2 simulated at Kashiru is not associated with the low partial pressure of CO_2 at high elevations. Increasing atmospheric pressure to 10^5 Pa (sea level) resulted in a small (4%) increase in the simulated net primary production (NPP). The change is small because the effect of the reduced partial pressure of CO_2 on photosynthesis at high elevation is partly compensated by the reduced partial pressure of O_2 (*27*). The simulated decrease in NPP obtained by reducing the CO_2 mixing ratio to 190 ppmv is still ≈35% at sea level if the mixing ratio of O_2 is held constant. Thus, effects of the low glacial CO_2 concentration on NPP are expected at all elevations. Lowering CO_2 levels increases stomatal conductance and therefore increases drought stress. This result implies that there may be even stronger direct CO_2 effects on biome distribution in more water-limited environments, such as tropical seasonal and dry forests. Still further responses may occur because C_3 plants (including almost all woody plants) are less competitive relative to C_4 grasses at low CO_2 concentrations (*14*).

The model predicts that the temperature range occupied by scrub increased as CO_2 decreased (Fig. 2), suggesting that the scrub belt would occupy a greater elevational range at low CO_2 concentrations. This pattern may explain the persistence of the scrub belt (ericaceous belt) for several thousand years around the LGM observed in the pollen record at altitudes of 1950 (*5*), 2200 (*8*, *28*), and 2400 m (*6*) in the East African mountains. Such stability might be attributed either to a uniform climate during this period, which is in contradiction with ice-core and North Atlantic sediment records (*29*), or to an expanded ecological range of this biome under low atmospheric CO_2 levels.

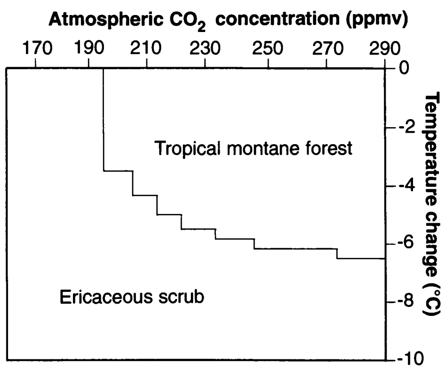

Fig. 2. Biomes simulated by BIOME3 at Kashiru for the present climate and with lowered temperatures and CO_2.

Our results do not conflict with the cooling and drying indicated by climate model simulations for the LGM (*2*, *3*). The existence of a direct CO_2 effect implies that there is no demonstrated inconsistency between the Indian Ocean sea surface temperature at the LGM, estimated to be 0° to 4°C lower than today, and the tree-line depression in East Africa (*30*). LGM climate reconstructions from paleovegetation data, using any approach based on present climate analogs, may be unreliable if they do not account for this direct CO_2 effect.

REFERENCES AND NOTES

1. A. J. Broccoli and S. Manabe, *Clim. Dyn.* **1**, 87 (1987); COHMAP Members, *Science* **241**, 1043 (1988).
2. D. Jolly *et al.*, *Quat. Sci. Rev.*, in press.
3. T. Webb III *et al.*, in *Global Climates Since the Last Glacial Maximum*, H. E. Wright *et al.*, Eds. (Univ. of Minnesota Press, Minneapolis, 1993), pp. 514–535.
4. D. M. Anderson and R. Webb, *Nature* **367**, 23 (1994).
5. A. C. Hamilton, *Environmental History of East Africa: A Study of the Quaternary* (Academic Press, New York, 1982).
6. J. A. Coetzee, *Palaeoecol. Afr.* **3**, 1 (1967).
7. D. A. Livingstone, *Ecol. Monogr.* **37**, 25 (1967).
8. R. Bonnefille and G. Riollet, *Quat. Res.* **30**, 19 (1988).
9. R. Bonnefille, J.-C. Roeland, J. Guiot, *Nature* **345**, 347 (1990).
10. R. Bonnefille *et al.*, *Clim. Dyn.* **6**, 251 (1992); A. Vincens et *al.*, *Quat. Res.* **40**, 343 (1993).
11. D. Rind, *Nature* **346**, 317 (1990).
12. G. M. Peterson *et al.*, *Quat. Res.* **12**, 47 (1979).
13. Atmospheric CO_2 concentration at the last glacial maximum was ~190 ppmv [J. M. Barnola *et al.*, *Nature* **329**, 408 (1987)].
14. A.-M. Aucour, C. Hillaire-Marcel, R. Bonnefille, *Quat. Res.* **41**, 225 (1994); F. A. Street-Perrott, *Ambio* **23**, 37 (1994).
15. A. Haxeltine and I. C. Prentice, *Glob. Biogeochem. Cycles* **10**, 693 (1996).
16. Model inputs were atmospheric CO_2 concentration, atmospheric pressure, latitude, soil texture, absolute minimum temperature, and mean monthly climate (temperature, precipitation, and sunshine). Model output consisted of a quantitative vegetation state description in terms of the dominant plant type, other plant types present, total leaf area and NPP, and a biome type based on this information. Where a dominant woody plant functional type was simulated, scrub biomes were distinguished from forest biomes on the basis of annual NPP (where NPP < 300 g C m^{-2} $year^{-1}$), in accordance with observations [H. Walter, *Vegetation of the Earth and Ecological Systems of the Geo-biosphere* (Springer-Verlag, New York, 1979)].
17. A. Haxeltine, I. C. Prentice, I. D. Cresswell, *J. Veg. Sci.* **7**, 651 (1996).
18. A. Haxeltine and I. C. Prentice, *Funct. Ecol.* **10**, 551 (1996).
19. J. Lewalle, *Bull. Jard. Bot. Natl. Belg.* **42**, 1 (1972).
20. R. Leemans and W. Cramer, *The IIASA Climate Da-*

tabase for Mean Monthly Values of Temperature, Precipitation & Cloudiness on a Terrestrial Grid (International Institute for Applied Systems Analysis, Laxenburg, Germany, 1991).
21. J. Lloyd and G. D. Farquhar, *Oecologia* **99**, 201 (1994).
22. I. C. Prentice *et al.*, *J. Biogeogr.* **19**, 117 (1992).
23. A preindustrial atmospheric CO_2 concentration of 280 ppmv was used [G. I. Pearman *et al.*, *Nature* **320**, 248 (1986); A. Neftel *et al.*, *ibid.* **331**, 609 (1988)].
24. J. F. Griffiths, *Climate of Africa* (Elsevier, Amsterdam, 1972).
25. O. Hedberg, *Sven. Bot. Tidskr.* **45**, 141 (1951).
26. A. C. Hamilton, *Palaeoecol. Afr.* **7**, 45 (1972); E. M. Van Zinderen Bakker, *ibid.* **14**, 77 (1982). Recent pollen analyses from lowland Amazonia have suggested an LGM temperature on the same order of 5° to 6°C [P. A. Colinvaux, P. E. De Oliveira, J. E. Moreno, M. C. Miller, M. B. Bush, *Science* **274**, 85 (1996)].
27. I. Terashima *et al.*, *Ecology* **76**, 2663 (1995).
28. D. Taylor, *Palaeogeogr. Palaeoclimatol. Palaeoecol.* **80**, 283 (1990).
29. W. Dansgaard *et al.*, *Nature* **364**, 218 (1993); G. Bond *et al.*, *ibid.* **365**, 143 (1993).
30. CLIMAP Project Members, *Geol. Soc. Am. Map Chart Ser. MC-36* (1981); D. Rind and D. Peteet, *Quat. Res.* **24**, 1 (1985).
31. Supported by the Swedish Natural Science Research Council (NFR) and by the U.S. Environmental Protection Agency under a subcontract with the University of New Hampshire in support of International Geosphere-Biosphere Program (IGBP) GAIM activities. This is a contribution to the (NSF) TEMPO, (European Union) PMIP, RUKWA, and (PNEDC) ERICA projects and to the core research of IGBP-GCTE. We thank I. C. Prentice and two anonymous reviewers for comments on the manuscript.

2 December 1996; accepted 10 March 1997

Surface Deformation and Lower Crustal Flow in Eastern Tibet

Leigh H. Royden,* B. Clark Burchfiel, Robert W. King, Erchie Wang, Zhiliang Chen, Feng Shen, Yuping Liu

Field observations and satellite geodesy indicate that little crustal shortening has occurred along the central to southern margin of the eastern Tibetan plateau since about 4 million years ago. Instead, central eastern Tibet has been nearly stationary relative to southeastern China, southeastern Tibet has rotated clockwise without major crustal shortening, and the crust along portions of the eastern plateau margin has been extended. Modeling suggests that these phenomena are the result of continental convergence where the lower crust is so weak that upper crustal deformation is decoupled from the motion of the underlying mantle. This model also predicts east-west extension on the high plateau without convective removal of Tibetan lithosphere and without eastward movement of the crust east of the plateau.

The topography and geology of the Tibetan region resulted from postcollision north-south convergence between the Indian and Eurasian plates since ~50 million years ago (Ma) (*1–3*) (Fig. 1). In this process, the Tibetan plateau was uplifted by >4 km and its crust thickened to twice normal thickness (~70 km) (*4–10*). Several competing models have been proposed for the uplift and deformation of Tibet, each with different implications for the eastern part of the Tibetan plateau (*11–17*). Here, we propose a model for the crustal dynamics within the plateau on the basis of geologic and Global Positioning System (GPS) observations of young crustal deformation along the eastern margin of the plateau.

Much of the eastern margin of the plateau lacks evidence for large-scale young crustal shortening; folds and thrust faults along the plateau margin are commonly oblique to and older than the plateau margin (*18*). In the Northern Longmen Shan, folds and faults trend east-west, nearly perpendicular to the plateau edge, and are mainly of Mesozoic age. In the south central Longmen Shan, the crust was probably shortened by ~100 km in Mio-Pliocene time, but there is no evidence for major Quaternary shortening. GPS results are consistent and constrain shortening across the Longmen Shan to be 0 ± 5 mm year^{-1} (*19, 20*). This lack of young deformation is surprising because the topographic front of the eastern plateau is as impressive as that of the Himalayas.

A similar mismatch between surface structure and topography occurs in the Yunnan region (south of the Xianshuihe fault). The active faults in this region cross from the high plateau into regions of lower elevation in southeast China (*19*). They are predominantly left-slip and trend south to southeast, nearly perpendicular to the plateau margin (Fig. 1B). Both geological and GPS results indicate slip on the Xianshuihe fault at ~20 mm year^{-1} (*19–21*). However, since 4 Ma or earlier, the southeastern corner of the plateau has rotated clockwise around the eastern Himalayan syntaxis with little, if any, net translation of upper crustal material eastward across or into the plateau margin (*19*). Thus, although we cannot rule out the possibility of eastward extrusion of Tibetan crust relative to Siberia in Pliocene-Quaternary time, there are no data to support this hypothesis, and, if extrusion occurs, southern China must be moving eastward at approximately the same rate as the central and southern parts of eastern Tibet.

Also noteworthy is the lack of a Cenozoic foredeep basin along the eastern margin of the plateau, which implies that the eastern foreland was not flexurally depressed during Cenozoic time. [Although the Sichuan basin is often considered to be a foredeep basin to the eastern plateau, rocks exposed in the basin are mainly Mesozoic in age. Where present, the Cenozoic cover is thin (≤200 m), and pre–Late Quaternary rocks are eroding throughout most of the Sichuan basin (*18*)]. A zone of extensional structures formed by margin-perpendicular extension of unknown Cenozoic age coincides with the topographically high mountains that rim the edge of the eastern plateau (*18*). These structures are reminiscent of the low-angle normal faults present along the northern margin of the Himalayas (*22*).

Various models of Cenozoic deformation within Tibet indicate that the uplift and surface deformation of the Tibetan plateau are intimately linked to the manner in which the crust beneath the plateau has been deformed at depth (*14, 15, 23–25*). However, these models do not match the observed surface deformation of Tibet in a number of important ways (*26*): They do not display east-west extension or eastward motions of the plateau (*26, 27*), they do not display large clockwise rotation of crustal material around the eastern Himalayan syntaxis (*19–21*), they do not reproduce margin-parallel extension along the plateau margin (*18*), and they do not offer a satisfactory explanation for the lack of surface shortening along the southeastern margin of the plateau (*18, 19*).

In two dimensions, quantitative studies of model convergent systems have shown that topography, strain partitioning, and degree of crust-mantle coupling are systematically related to the strength (viscosity) of the crust as a function of increasing depth (*25, 28, 29*). In particular, steep-sided flat-topped plateaus develop only when a low-viscosity zone is absent beneath the foreland and the margins of the plateau but is present in regions of thickened crust beneath the plateau proper. Because recent studies suggest that the lower crust beneath Tibet may be weak (*30, 31*), some of the inadequacies in the thin viscous sheet models may occur because such models ignore depth-dependent behavior and thus cannot incorporate lateral shear

L. H. Royden, B. C. Burchfiel, R. W. King, E. Wang, Department of Earth, Atmospheric, and Planetary Sciences, Massachusetts Institute of Technology, Cambridge, MA 02139, USA.
Z. Chen, F. Shen, Y. Liu, Chengdu Institute of Geology and Mineral Resources, Chengdu, China.

*To whom correspondence should be addressed.